

Xin ZHANG
Jianmin ZHAO

COMPOUND FAULT DETECTION IN GEARBOX BASED ON TIME SYNCHRONOUS RESAMPLE AND ADAPTIVE VARIATIONAL MODE DECOMPOSITION

WYKRYWANIE ZŁOŻONYCH BŁĘDÓW PRZEKŁADNI NA PODSTAWIE SYNCHRONICZNEGO PRÓBKOWANIA WTÓRNEGO ORAZ ADAPTACYJNEJ METODY WARIACYJNEJ DEKOMPOZYCJI MODALNEJ

Compound fault detection of gearboxes is an ambitious matter considering its interconnection and complication. An innovative means for compound fault detection based on time synchronous resample (TSR) and adaptive variational mode decomposition (AVMD) is put forward in this work. TSR used in the method can enhance fault signals of synchronous shaft gears by eliminating signal components independent of synchronous shaft. Therefore, the TSR is used to separate the synchronous shaft signal corresponding to the gear fault from the raw compound fault signal. Then a series of mode components are obtained by decomposing the synchronous shaft signals of all faults by AVMD. The variational mode decomposition (VMD) can overcome the mode aliasing problem of empirical mode decomposition (EMD), but the decomposition effect of VMD is affected by its parameter setting. Thus, the paper proposes an AVMD algorithm based on whale optimization algorithm (WOA). In the AVMD, the WOA is used to optimize the parameters of the VMD. After AVMD decomposition, the correlated kurtosis of the mode components obtained by AVMD decomposition is calculated. Then the mode components with the maximum correlated kurtosis are selected to carry out envelope analysis. Finally, the compound fault feature can be found from the envelope spectrum to get the diagnosis results. In order to test the validity of the proposed method, a compound fault experiment is implemented in a gearbox. Through the analysis of the experimental data, it is proved that the method shows a good performance in the compound fault detection of gearbox.

Keywords: compound fault; gearbox; time synchronous resample; adaptive variational mode decomposition.

Wykrywanie złożonych błędów przekładni stanowi trudne zagadnienie ze względu na ich skomplikowany charakter i powiązania wewnętrzne. W pracy zaproponowano nowatorską metodę wykrywania błędów złożonych opartą na synchronicznym próbkowaniu wtórnym (TSR) oraz adaptacyjnej metodzie wariacyjnej dekompozycji modalnej (AVMD). TSR pozwala wzmocnić sygnały błędów występujących w synchronicznych przekładniach walcowych, dzięki eliminacji składowych sygnałów niezwiązanych z działaniem wału synchronicznego. Dlatego też w przedstawionych badaniach, TSR wykorzystano do wyodrębnienia sygnału wału synchronicznego odpowiadającego błędowi przekładni, z surowego sygnału błędu złożonego. Następnie wszystkie sygnały błędów wału synchronicznego poddano dekompozycji za pomocą AVMD, dzięki czemu otrzymano szereg składowych modalnych. Wariacyjna dekompozycja modalna (VMD) pozwala uniknąć problemu aliasingu, który występuje w przypadku empirycznej dekompozycji modalnej (EMD), przy czym efekt dekompozycji zależy od ustawień parametrów. Dlatego w artykule zaproponowano adaptacyjny algorytm VMD oparty na algorytmie optymalizacji wielorybów (WOA), który optymalizuje parametry VMD. Następnym krokiem po dekompozycji AVMD, było obliczenie skorelowanej kurtozy składowych modalnych otrzymanych na drodze tej dekompozycji. Składniki modalne o najwyższych wartościach skorelowanej kurtozy wykorzystano do przeprowadzenia analizy obwiedni. Błąd złożony wykrywano na podstawie widma obwiedni. Skuteczność proponowanej metody sprawdzono przeprowadzając doświadczenie na przekładni, w której występował błąd złożony. Wyniki eksperymentu pokazują, że proponowane podejście stanowi skuteczną metodę wykrywania złożonych błędów.

Słowa kluczowe: błąd złożony; przekładnia; synchroniczne próbkowanie wtórne; adaptacyjna metoda wariacyjnej dekompozycji modalnej.

1. Introduction

Gearboxes are vital elements that are extensively used in automobile, aeroplanes and energy equipment. The gearboxes fault account for 80% in the shutdown malfunction of the transmission machinery[20, 22]. Therefore, it is essential to carry out gearbox fault diagnosis to prevent the gearbox from malfunction and reduce the economic loss[27]. Due to the long running time and poor working conditions, the faults of gearbox often occur in the form of compound fault simultaneously. Compound fault of gearbox may cause more serious consequences or unnecessary economic losses in maintenance activities. Thus, it is essential to develop the study on compound fault detection technology of gearbox. At present, the compound fault vi-

bration signals collected from gearbox usually have the following characteristics: (a) In the original signal collected from the gearbox, the fault component belongs to the weak signal buried in the strong signal such as gear meshing component and noise; (b) Various faults may exist at the same time and interfere with each other. This causes the fault signal to be more complex and non-stationary[4]. Therefore, the above characteristics make it inconvenient to diagnose the compound fault of gearboxes.

At present, many technologies have been introduced to compound fault diagnosis of gearbox. Guo et al.[6] put forward the gear vibration model for the planetary gear compound fault detection. Nevertheless, owing to the non-linearity, non-stationarity and complexity of

the compound fault signal and the complexity of the internal structure of the gearbox, it is laborious to raise an available model for compound fault detection. Blind Source Separation (BSS) algorithm has been applied to compound fault diagnosis of rotating machinery[7, 15], but the high requirement for raw signals limits the application of BSS algorithm. The sparse decomposition[31], spectral kurtosis[1] and morphological component analysis[30, 3] have also been introduced for compound fault detection of gearbox and have shown good performance. Wavelet transform (WT) is a commonly used and effective time-frequency analysis method. So many scholars have been put forward some compound fault diagnosis methods of gearbox based on WT. Purushotham et al.[19] proposed a compound fault means for rolling bearing based on WT. Similarly, many improved wavelet transforms have been proposed and introduced for compound fault detection, such as multiwavelet transform[13, 8], multiwavelet packet transform[25, 11], dual-tree complex wavelet transform[21, 26, 28] and empirical wavelet transform[5, 12]. However, the selection of wavelet basis function will determine the performance of WT, which is also a major disadvantage of WT. As an adaptive time-frequency analysis method, empirical mode decomposition[10] (EMD) can adaptively decompose the signal into a certain number intrinsic mode functions satisfying certain conditions. EMD is suitable for processing nonlinear and non-stationary signals because of its self adaptability. For this reason, EMD is introduced into the analysis of gearbox mixed fault signal, which have shown good performance[9]. But the EMD has the disadvantage of mode aliasing, which will affect the effect of compound fault feature extraction. The ensemble empirical mode decomposition (EEMD) is an improved signal analysis method based on EMD, which can alleviate the disadvantages of modal aliasing in EMD[29]. Sandip et al.[23] have put forward a compound fault detection approach based on EEMD and Convolution Neural Networks (CNN)[33]. It is found that there is still a certain degree of modal aliasing in EEMD and the method is sensitive to the noise existing in the signal[18]. The local mean decomposition (LMD) was proposed by Jonathan S. Smith and has been used to analyze electroencephalogram signal[24]. Jiao et al. carried out multi-faults diagnosis of rotor system using LMD-based time-frequency representation. However, LMD still has a certain degree of mode aliasing, which affects the diagnostic results.

The variational mode decomposition (VMD) method is a novel adaptive signal processing method proposed by Konstantin Dragomiretskiy[32]. It can overcome some shortcomings of EMD, such as mode aliasing and endpoint effect. VMD is completely different from the recursive decomposition algorithm of EMD. Its overall framework is a constrained variational problem and has a solid theoretical foundation. The VMD suppose that each mode element is closely surrounded by a central frequency, and transforms determination of mode bandwidth into a constrained variational problem. Separation of mode elements is achieved by solving the constrained variational problem. VMD can segment the signal frequency domain flexibly and extract the latent feature information effectively. The number of mode components and penalty factors are two critical parameters of VMD, which can influence the performance of VMD in decomposition signal. The better decomposition results of VMD need appropriate parameters. Aiming at this problem, the paper proposes an adaptive variational mode decomposition (AVMD) algorithm based on whale optimization algorithm (WOA). WOA is a new intelligent optimization algorithm put forward by Mirjalili[17], which imitates the hunting strategy of humpback whales. The advantages of WOA algorithm include less parameter settings and fast optimization speed.

In addition, the raw vibration signals collected from gearbox often contain noise and other interference signals besides fault signals[14]. Compared with other interference signals, fault signals belong to weak signals. Therefore, it is necessary to preprocess the original signal and enhance the fault signal. Time synchronous average (TSA)[2]

is an effective technique in signal preprocessing for gearbox. TSA can enhance fault signals of synchronous shaft gears and their meshing gears by eliminating signal components independent of synchronous shaft, such as bearing vibration, motor vibration, gear meshing vibration independent of synchronous shaft and vibration from other mechanical equipment[16]. However, TSA will filter out the bearing fault signal in gearbox, and the signal length will be greatly shortened after the average synchronization, so the algorithm has requirements on the signal length. Therefore, a signal preprocessing method based on TSR is presented in this work.

The remainder of this article is arranged as follows. The fundamental theory of the proposed method is elaborated in the Section 2. In Section 3, the procedure of AVMD is presented. The flow chart of compound fault detection approach based on TSR-AVMD is illustrated in the Section 4. In Section 5, the performance of TSR-AVMD is validated by using compound fault experimental data of gearbox, and results are compared with other methods. The conclusions are given in the Section 6.

2. Materials and Methods

2.1. Time synchronous resample

For continuous signal $g(t)$, if it satisfies the Dirichlet condition, its Fourier transform is shown as follows:

$$X(\omega) = \int_{-\infty}^{+\infty} g(t) \exp(-i\omega t) dt \quad (1)$$

Further assume that the signal is a limited bandwidth signal:

$$X(\omega) = 0 \quad |\omega| > 2\pi f_g \quad (2)$$

The sampling frequency band $\{z(p)\}$ can be obtained by sampling the signal $g(t)$ at the starting time t_z with the sampling frequency $f_s > 2f_g$:

$$z(p) = g\left(\frac{p}{f_s} - t_z\right) \quad p = 0, 1, \dots, p-1 \quad (3)$$

where t_z is the beginning time of sampling.

N data segments of R sampling points can be obtained through the same method:

$$x_n(r) = g\left(\frac{r}{f_s} - t_n\right) \quad r = 0, 1, \dots, R-1 \quad n = 0, 1, \dots, N-1 \quad (4)$$

where t_n is the sampling beginning time of the n th sampling data segment, and N is called the average segment number. If it is assumed that the start times of these data segments correspond to the same signal flag, and these data segments are synchronized, then new data segments can be obtained on average for these data segments:

$$y(r) = \frac{1}{N} \sum_{n=0}^{N-1} x_n(r) \quad r = 0, 1, \dots, R-1 \quad (5)$$

where $y(r)$ is called time synchronized averaging signal, and the above procedure is called time synchronous average. But after TSA processing, the signal related to bearing fault will be filtered out, and the bearing fault in gearbox cannot be detected. In addition, the length of signal is greatly reduced after TSA processing, which affects the

subsequent analysis. For this reason, the input signal of TSA needs enough length, which limits the application of this technology. Therefore, this paper only carries out synchronous resampling without average processing to overcome these shortcomings, which is called time synchronous resample.

2.2. Variational mode decomposition

The theory of VMD will be illustrated in this section. The intrinsic mode function in VMD refers to an amplitude modulation-frequency modulation signal, which is shown as follows:

$$u_k(t) = A_k(t) \cos(\varphi_k(t)) \tag{6}$$

where $A_k(t)$ indicates the signal amplitude, $\varphi_k(t)$ is the phase of the signal. $\omega_k(t) = \frac{d\varphi(t)}{dt}$ stands for instantaneous frequency. The mode

mentioned here is assumed to be a finite bandwidth component with a central frequency. The VMD is to seek the intrinsic mode function, which the sum of K estimation bandwidth is the smallest. The constraint condition is the sum of IMFs equal to the primary signal $f(t)$. The specific measures to constructing constrained variational models are shown below:

Hilbert transform is performed for each IMF, as shown in the following formula:

$$\left(\delta(t) + \frac{j}{\pi t} \right) * u_k(t) \tag{7}$$

For each IMF component, the corresponding center frequency ω_k is estimated and multiplied with the exponent signal $e^{-j\omega_k t}$, and the corresponding mode spectrum of each fundamental band is modulated:

$$\left(\delta(t) + \frac{j}{\pi t} \right) * u_k(t) e^{-j\omega_k t} \tag{8}$$

The square of the norm of the gradient L^2 above the modulation signal is calculated. The bandwidth of each IMF component is evaluated. The following constraint variational model is constructed:

$$\begin{cases} \min_{\{u_k\}, \{\omega_k\}} \left\{ \sum_{k=1}^K \left\| \partial_t \left[\left(\delta(t) + \frac{j}{\pi t} \right) * u_k(t) \right] e^{-j\omega_k t} \right\|_2^2 \right\} \\ s.t. \sum_{k=1}^K u_k(t) = f(t) \end{cases} \tag{9}$$

where $\delta(t)$ is unit impulse function, j is imaginary unit, $*$ indicates the convolution operation, ∂_t indicates partial derivation of functions, $\{u_k\} = \{u_1, u_2, \dots, u_K\}$ indicates the decomposed K IMFs elements. $\{\omega_k\} = \{\omega_1, \omega_2, \dots, \omega_K\}$ represents the central frequency of each IMF component.

To solve the problem of Eq (9), penalty factor α and Lagrange multiplier λ are introduced to transform the constrained variational problems into unconstrained ones. The augmented Lagrange expression is obtained in the following form:

$$L(\{u_k\}, \{\omega_k\}, \lambda) = \alpha \sum_{k=1}^K \left\| \partial_t \left[\left(\delta(t) + \frac{j}{\pi t} \right) * u_k(t) \right] e^{-j\omega_k t} \right\|_2^2 + \left\| f(t) - \sum_{k=1}^K u_k(t) \right\|_2^2 + \left\langle \lambda(t), f(t) - \sum_{k=1}^K u_k(t) \right\rangle \tag{10}$$

The alternate direction method of multipliers are used to iteratively update u_k , ω_k and λ to search the saddle point of augmented Lagrange expression. Specific implementation steps are shown as follows:

- (1) Initialize the $\{\hat{u}_k^1\}, \{\omega_k^1\}, \hat{\lambda}^1, n$
- (2) Repeat cycle: $n=n+1$
- (3) For all $\omega \geq 0$, update the $\hat{u}_k, \omega_k, \hat{\lambda}$

$$\hat{u}_k^{n+1}(\omega) = \frac{\hat{f}(\omega) - \sum_{i=1}^{k-1} \hat{u}_i^{n+1}(\omega) - \sum_{i=k+1}^K \hat{u}_i^n(\omega) + \frac{\hat{\lambda}^n(\omega)}{2}}{1 + 2\alpha(\omega - \omega_k^n)^2} \tag{11}$$

$$\omega_k^{n+1} = \frac{\int_0^\infty \omega |\hat{u}_k^{n+1}(\omega)|^2 d\omega}{\int_0^\infty |\hat{u}_k^{n+1}(\omega)|^2 d\omega} \tag{12}$$

$$\hat{\lambda}^{n+1}(\omega) = \hat{\lambda}^n(\omega) + \tau \left(\hat{f}(\omega) - \sum_{k=1}^K \hat{u}_k^{n+1}(\omega) \right) \tag{13}$$

- (4) Repeat the (2) and (3) steps unless the iteration termination condition is met.

$$\sum_{k=1}^K \left(\left\| \hat{u}_k^{n+1}(\omega) - \hat{u}_k^n(\omega) \right\|_2^2 / \left\| \hat{u}_k^n(\omega) \right\|_2^2 \right) < \varepsilon \tag{14}$$

End the iteration and get K IMFs components.

2.3. Theory of whale optimization algorithm

The whale optimization algorithm is an innovative intelligent optimization algorithm which is mainly formed by simulating the process of humpback whale's predation. The predatory behavior of humpback whales can be summarized as the following three behaviors: randomly searching for prey, surrounding target prey and preying on target prey. In WOA, the position of each humpback whale is expressed as a feasible solution to the research problem.

2.3.1. Randomly searching for prey

Searching for a feasible solution to a problem can be modeled on the process of whale swarm randomly searching for target prey. The mathematical model is as follows:

$$\mathbf{X}_{j+1} = \mathbf{X}_{rand} - \mathbf{A} \times \mathbf{D} \tag{15}$$

$$\mathbf{D} = \left| \mathbf{C} \times \mathbf{X}_{rand} - \mathbf{X}_j \right| \tag{16}$$

where j is the current number of iterations, \mathbf{A} and \mathbf{C} are coefficient vectors, \mathbf{X}_{rand} is the position vector randomly selected from the current whale group, which is the possible solution.

The \mathbf{A} and \mathbf{C} in Eq. (15) and Eq. (16) can be obtained as follows:

$$\mathbf{A} = 2\mathbf{a} \times \mathbf{r}_1 - \mathbf{a} \tag{17}$$

$$C = 2\mathbf{r}_2 \quad (18)$$

where \mathbf{a} is a vector that falls linearly from 2 to 0, the \mathbf{r}_1 and \mathbf{r}_2 are random vectors in the range 0 to 1.

2.3.2. Surrounding target prey

The process of humpback whales approaching the target prey can be seen as the process of approaching the feasible solution in the algorithm. If the target prey is the best individual location for the current population, the location will be updated as follows:

$$\mathbf{X}_{j+1} = \mathbf{X}_j - \mathbf{A} \times \mathbf{D} \quad (19)$$

$$\mathbf{D} = \left| C \times \mathbf{X}_j^* - \mathbf{X}_j \right| \quad (20)$$

where \mathbf{X}_j is the position vector of current whale, \mathbf{X}_j^* is currently the best whale position vector.

2.3.3. Preying on target prey

Humpback whales prey on the target through the following two strategies:

1. Shrinking encircling mechanism: This mechanism is realized by reducing the value of a , where a is a random value between $[-2, 2]$; When a is in the range of $[-1, 1]$, the position the whales are looking for is the position of the target prey. At this time, the whale group is close to the target prey, on the contrary, whales stay away from the prey.
2. Spiral updating position: The humpback whales approach their prey in a spiral motion. According to the motion mode, a mathematical model can be constructed as follows:

$$\mathbf{X}_{j+1} = \mathbf{D}' e^{bl} \cos(2\pi l) + \mathbf{X}_j^* \quad (21)$$

where $\mathbf{D}' = \left| \mathbf{X}_j^* - \mathbf{X}_j \right|$ is the distance between the current best position of the i th whale group and its prey, b is a constant for defining the shape of the logarithmic spiral, l is a random number in $[-1, 1]$.

The above two mechanisms are carried out at the same time in the process of whale predation. In order to simulate this situation, a 50% probability is selected between them to update the position of the whale group. It can be realized by the following mathematical model:

$$\mathbf{X}_{j+1} = \begin{cases} \mathbf{X}_j - \mathbf{A} \times \mathbf{D} & p < 0.5 \\ \mathbf{D}' e^{bl} \cos(2\pi l) + \mathbf{X}_j^* & p \geq 0.5 \end{cases} \quad (22)$$

where p is a random number in $[0, 1]$.

2.4. Adaptive variational mode decomposition

The procedure of AVMD is illustrated in this section. According to the description of VMD in the previous section, the number of components K and the penalty factor α are two critical parameters that influence the decomposition effect of VMD. If the value of K is much smaller than the number of natural modes of the signal, all modes in the signal will not be separated completely. On the contrary, some modal components in the signal may be over decomposed and finally some non-existent modes will appear. The penalty factor α mainly affects the bandwidth of the mode components decomposed by VMD. If the penalty factor is too small, the spectrum of component will be very wide, and the mode aliasing problem will occur easily. Conversely, the bandwidth of the component is narrowed, and the information contained in

the mode component may be insufficient. At present, the determination of the above two parameters mainly depends on human subjective experience, which may lead to unsatisfactory decomposition effect of VMD. Therefore, this paper proposes an AVMD, which employs the WOA to optimize the parameters of VMD.

A fitness function must be determined when using WOA to optimize influence parameters of VMD. The fitness function values under different parameters are calculated, and the influence parameters are selected and updated by comparing fitness function values. The fitness function is the maximum correlation kurtosis of modes received by VMD decomposition. Correlated kurtosis can detect the existence of periodic impact signals. In engineering practice, the original signal collected from the equipment contains some noise impact signals, which is not periodic. However, the traditional kurtosis can only reflect the impact characteristics of the signal. The traditional kurtosis may reflect only the impact signal of the noise rather than the fault impact signal. Therefore, the correlated kurtosis is used to select the IMF which contains fault impact component. The first order correlated kurtosis can be computed as follows:

$$CK_1(\tau) = \frac{\sum_{t=1}^N (y(t)y(t-\tau))^2}{\left(\sum_{t=1}^N y(t)^2\right)^2} \quad (23)$$

where the $y(t)$ is the vibration signal, τ represents the sampling point length corresponding to the fault frequency to be detected. The M -orders correlated kurtosis can be get as follows:

$$CK_M(\tau) = \frac{\sum_{t=1}^N (\prod_{m=0}^M y(t-m\tau))^2}{\left(\sum_{t=1}^N y(t)^2\right)^{M+1}} \quad (24)$$

The first order correlation kurtosis is mainly suitable for detecting early faults, and high order correlation kurtosis is mainly suitable for detecting serious faults.

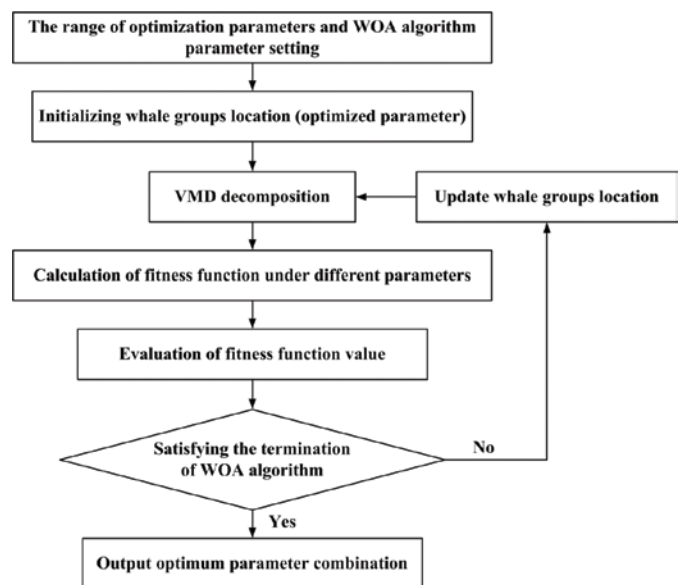


Fig. 1. Frame diagram of the AVMD

The Fig. 1 is presented the flow path of AVMD. Firstly, the optimization range for parameters and WOA algorithm parameters are set, and then the whale groups locations (optimization parameters) are initialized. Then VMD decomposition is performed to get a series of mode components. Then the fitness function is calculated, and the optimal results are chosen by evaluating fitness function. Finally, output optimization parameters when the termination condition of WOA is satisfied, otherwise the parameters are updated to continue the above operation.

2.5. Compound fault diagnosis method based on TSR-AVMD

A compound fault detection approach based on TSR-AVMD is presented in this work. The process of the proposed approach is illustrated in this section. The compound fault signals collected from gearbox include not only compound fault components, but also motor vibration signal, gear meshing vibration signal and vibration signal from other machinery and equipment. These irrelevant signals will affect the efficiency of compound fault diagnosis, so the TSR is introduced to process the original signal in this paper. TSR can enhance the fault signal of synchronous shaft gear and its meshing by removing the frequency component independent of synchronous shaft, which makes it easy to detect the fault located in synchronous shaft gear. To get the fault features and overcome the limitations of traditional VMD methods, AVMD is put forward to extract gear fault characteristic. The flow chart of proposed method for hybrid fault detection is shown as Fig. 2. The specific steps are described as follows.

- (1) Collect the original signal from the gearbox through the vibration acceleration sensor.
- (2) The original vibration signal is preprocessed by TSR technology, which enhances the synchronous shaft signal of each fault and eliminates the interference of the non-synchronous shaft signal component.
- (3) A series of mode components are obtained by decomposing the synchronous shaft signals of all faults by AVMD.
- (4) Calculate the correlated kurtosis of the mode components obtained by AVMD decomposition for all the fault synchronous

shaft signals. Then the mode components with the maximum correlated kurtosis are selected for the next step.

- (5) Finally, the envelope analysis of mode components with maximum correlation kurtosis is performed, and the envelope spectrum is obtained to realize fault detection.

3. Experimental analysis

The performance of the proposed method is testified by using experiment signal of compound fault of gearbox in this section. The setup of the experiment is illustrated in the follows.

3.1. Experimental setup

The structure of the experimental platform is shown in the Fig. 3. The experimental data is collected by the acceleration sensor installed on the gearbox. The structure of the test gearbox and the specific layout of four acceleration sensors are shown as Fig 4. In this experiment, there are 1mm crack fault in Gear 1 and 2mm broken tooth fault in Gear 2 which is preset in the gearbox. The location of the gear fault is shown in the Fig. 5. In the experiment, the motor speed is set to 1200rpm and the load is set to 20nm. The sampling frequency of data is 20kHz.

3.2. Experimental result analysis

The experimental data of 1mm crack fault in Gear 1 and 2mm broken tooth fault in Gear 2 is employed to test the validity of proposed method. The wave form of raw compound fault signal is presented in the Fig 6. The rotational speed of input shaft is 2000rpm. According to the gear parameters shown in the Fig.4, the rotational frequency of output shaft and intermediate shaft is 2.43Hz and 10.94Hz respectively. The two gears with crack fault and broken tooth fault are located in the output shaft and intermediate shaft respectively, so the corresponding fault frequencies of the two faults are 2.43Hz and 10.94Hz respectively.

The proposed approach is employed to perform the compound fault data. Firstly, the original data is preprocessed by TSR. The interference of signal components independent of synchronous axis is eliminated, and the synchronous shaft signals corresponding to crack fault and broken tooth fault are obtained respectively. Then the WOA is employed find the optimal parameters of VMD. The parameter settings of WOA are shown in the Table 1. Fig 7 shows the change curve of fitness function during the iteration of parameter optimization with WOA. As can be seen from the Fig 7 (a), the fitness is stable when the number of iterations reaches 7 generations, which shows that the optimal solution is found for broken tooth fault signal. Similarly, the optimal solution for crack fault is found when the number of iterations reaches 16 generations as shown in the Fig 7 (b). Thus, the optimal parameters of VMD are found, and the result is presented in Table 2. VMD decomposition of synchronous shaft signal corresponding to crack fault and broken tooth fault is carried out respectively. The VMD decomposition result of synchronous shaft signal corresponding to broken tooth fault and crack fault is presented in the Fig 8 and Fig 9 respectively. Then the correlated kurtosis of all mode components is computed and the modes with maximum correlated kurtosis are chosen for envelope analysis. The IMF with maximum 15 orders correlated kurtosis for synchronous shaft signal corresponding broken tooth fault is the second IMF, and the IMF with maximum 4 orders correlated kurtosis for synchronous shaft signal corresponding gear crack fault is the first IMF. The envelope spectrums of above two IMFs are obtained as presented in Fig 10.

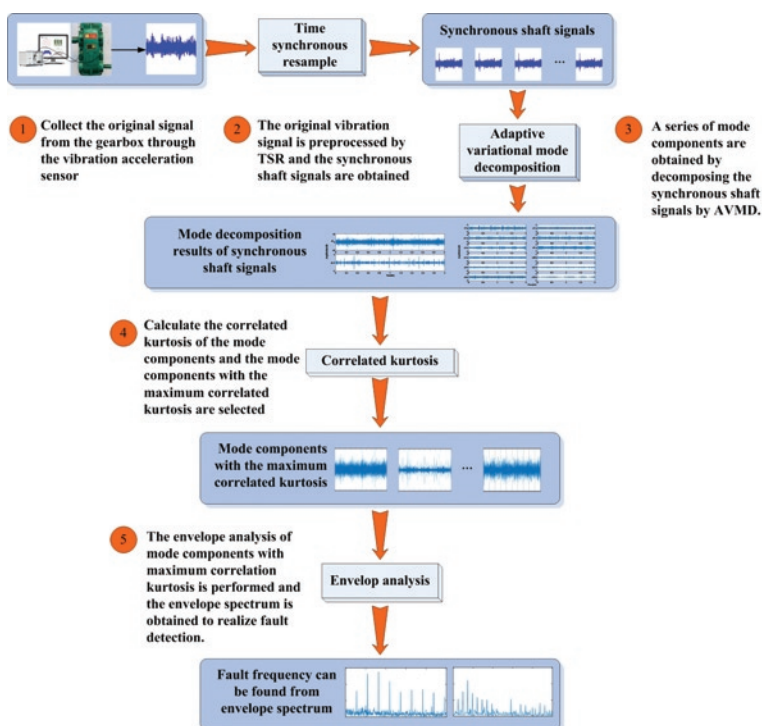


Fig. 2. Procedure of proposed method for compound fault detection

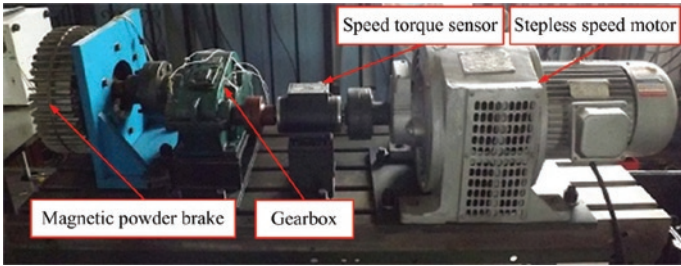


Fig. 3. Structure diagram of test rig

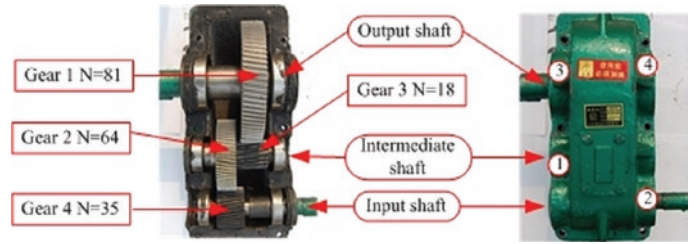


Fig. 4. Gearbox structure and sensor position



Fig. 5. Location of compound fault in gears

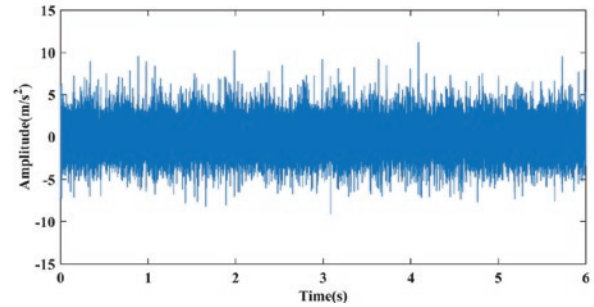


Fig. 6. The wave form of raw signal

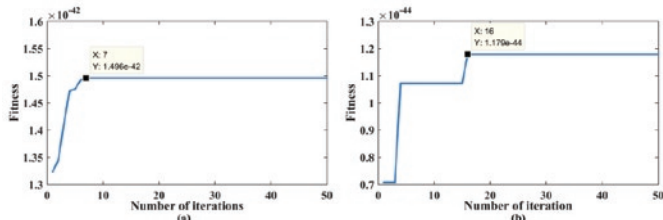


Fig. 7. The iterative process of optimization (a) iterative process for broken tooth fault signal (b) iterative process for crack fault signal

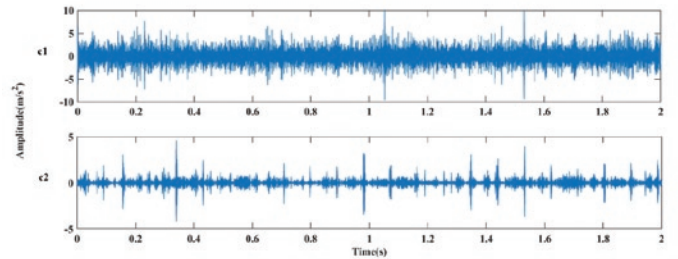


Fig. 8. Decomposition result of AVMD for synchronous shaft signal corresponding broken tooth fault

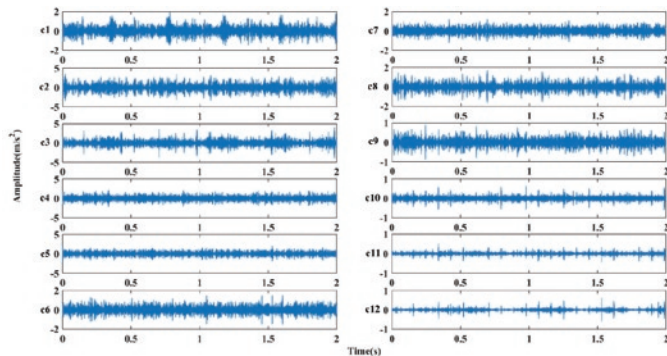


Fig. 9. Decomposition result of AVMD for synchronous shaft signal corresponding gear crack fault

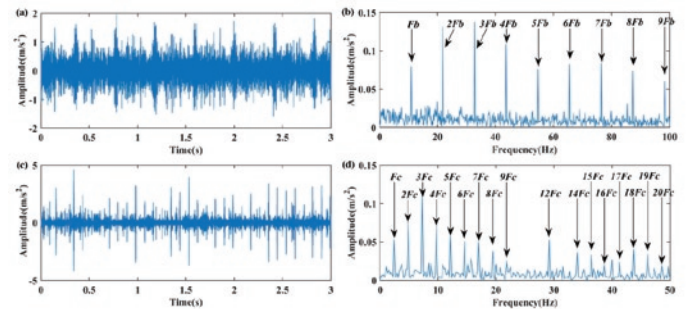


Fig. 10. The diagnosis results obtained by proposed method (a) IMF of signal with broken tooth fault (b) IMF of signal with gear crack fault (c) IMF of signal with gear crack fault; (b) & (d) The envelop spectrum of (a) and (c)

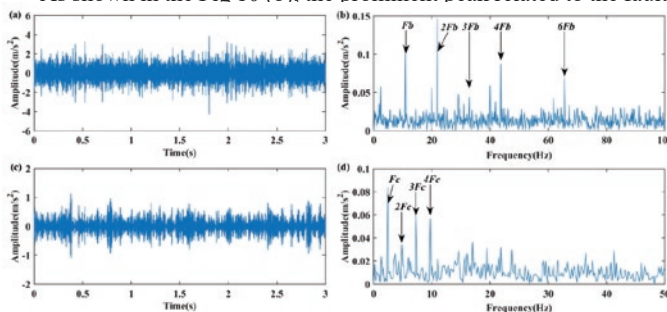


Fig. 11. Diagnosis results obtained by TSR-EMD (a) IMF of signal with broken tooth fault (c) IMF of signal with gear crack fault; (b) & (d) Envelop spectrum of (a) and (c)

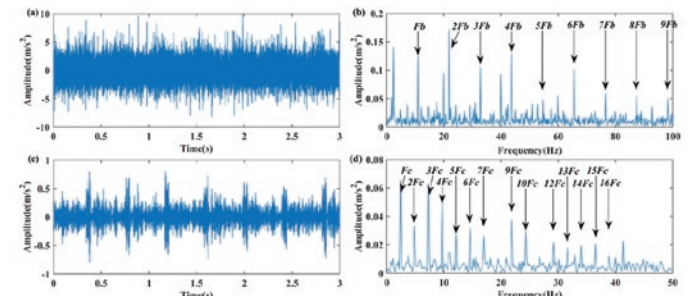


Fig. 12. Diagnosis results obtained by TSR-EEMD (a) IMF of signal with broken tooth fault (c) IMF of signal with gear crack fault; (b) & (d) Envelop spectrum of (a) and (c)

Table 1. Initial parameter settings of WOA

Number of search agents	Maximum generations	Number of parameters to be optimized	Floor of parameter K	Toplimit of parameter K	Floor of parameter α	Toplimit of parameter α
100	50	2	2	15	1000	10000

Table 2. Optimal parameters of VMD for different fault

K of VMD for broken tooth fault	K of VMD for gear crack fault	α of VMD for broken tooth fault	α of VMD for gear crack fault
2	12	7248	9247

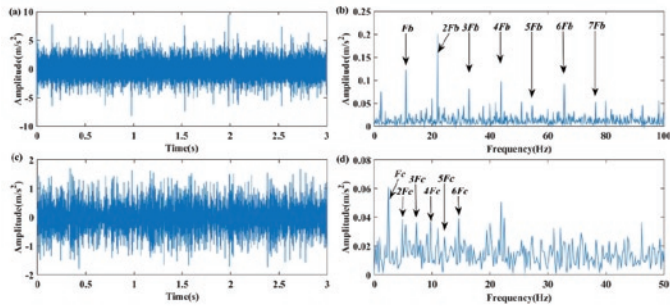


Fig. 13. Diagnosis results obtained by TSR-LMD (a) IMF of signal with broken tooth fault (c) IMF of signal with gear crack fault; (b) & (d) Envelop spectrum of (a) and (c)

frequency of broken tooth (F_b) and its harmonics can be identified evidently. As shown in the Fig 10 (d), the prominent peak corresponding to the fault characteristic frequency of crack (F_c) and its harmonics are evident clearly. In conclusion, the TSR-AVMD is able to separate the compound fault of broken tooth and gear crack in different shaft, and the corresponding fault can be detected effectively.

4. Discussion

In order to prove that the performance of TSR-AVMD is better than that of traditional methods, the EMD, EEMD and LMD are employed to perform the same data. Firstly, the compound fault signal is decomposed into a series of IMFs by using EMD, EEMD and LMD respectively. Then the IMFs with maximum 15 orders correlated kurtosis and maximum 4 orders correlated kurtosis are selected from the decomposition results. Finally, the selected IMFs which contains different gear fault are carried out envelope analysis and the envelope spectrums are shown in the Fig 11, Fig 12 and Fig 13.

As for envelop spectrum shown in the Fig 11 (b), the peak related to F_b is identified clearly. Partial harmonics of F_b appear in envelope spectrum, but compared to Fig 10 (b), the harmonic of some F_b is annihilated by other interference components. As for envelop spectrum presented in the Fig 11 (d), the prominent peak related to the F_c and its harmonics are identified, but not clearly. In the envelop spectrum, there are many interference components around F_c and its harmonics compared with Fig 10 (d). It shows that the performance of TSR-AVMD is more competitive than the TSR-EMD.

As shown in the Fig 12 (b), the peak related to F_b and its harmonics are identified. But in the spectrum, there are some interference components around F_b and its harmonics compared with the Fig 10 (b). In the Fig 12 (d), the peak related to F_c and its harmonics are identified clearly. It shows that the TSR-EEMD can detect the gear crack fault clearly. Nevertheless, the fault frequency of broken tooth cannot be extracted clearly enough, there are some interference components around F_b and its harmonics.

As for envelop spectrum shown in the Fig 13 (b), the peak related to F_b and its harmonics can be found, but there are disturbing components near the harmonics. It can be seen from the Fig 13 (d), the

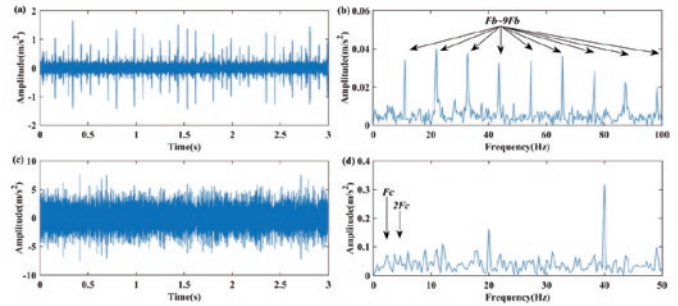


Fig. 14. Diagnosis results obtained only using AVMD (a) IMF of signal with broken tooth fault (c) IMF of signal with gear crack fault; (b) & (d) Envelop spectrum of (a) and (c)

peak related to F_c and its harmonics are disturbed seriously. It shows that the TSR-LMD can detect the broken tooth fault, and the performance of TSR-AVMD is more competitive than the TSR-LMD. But the TSR-LMD cannot detect the gear crack fault effectively.

In conclusion, the performance of TSR-AVMD in compound fault detection is more competitive than the TSR-EMD, TSR-EEMD and TSR-LMD.

To prove the necessity of TSR in the presented approach, the AVMD is employed alone to analyze the raw signals that are not processed by TSR. Then the envelop spectrums of IMFs with 15 orders maximum correlated kurtosis and 4 orders maximum correlated kurtosis are shown as Fig 14. As shown in the Fig 14 (b), the prominent peak related to the fault frequency of broken tooth (F_b) and its harmonics are clearly identified. However, the prominent peak related to the characteristic frequency of crack (F_c) and its harmonics cannot be found in the Fig 14 (d) clearly. Thus, the gear broken tooth fault can be detected and the gear crack fault cannot be detected. In summary, it shows that the gear crack fault cannot be detected by only using AVMD, and it proves the necessity of the TSR in the proposed method.

5. Conclusions

An innovative compound fault detection approach based on TSR and AVMD is presented in this paper. In the implementation of the presented approach, the TSR is used to preprocess the raw signal to eliminate the interference of asynchronous shaft signal. Then the AVMD is employed to process the fault synchronous shaft signals obtained by TSR to extract fault features. The AVMD introduces WOA to optimize the main parameters of VMD, which overcomes the problem that the decomposition effect of VMD is affected by parameters. Then the optimal mode components that represent the fault features of gears are selected based on the principle of the maximum correlated kurtosis. Finally, the compound fault features can be extracted from the envelop spectrum of the optimal mode components. The compound fault experiment of gearbox is performed to test the validity of the TSR-AVMD. After the analysis and comparison of the experimental results, the following conclusions can be obtained.

- (1) TSR is an available approach for extracting synchronous shaft fault signals and eliminating other interference signals. The experimental results show that TSR can eliminate the interference of non-synchronous shaft signal and enhance the fault signal of gearbox.
- (2) AVMD can effectively overcome the shortcomings of mode aliasing in EMD. Through comparative analysis of experimental results, it can be proved that the performance of extracting fault features by AVMD is more competitive than traditional time frequency analysis methods such as EMD, EEMD and LMD.
- (3) Through the experiment of compound faults in gearbox, the compound fault detection approach based on TSR and AVMD presented in this work can detect compound faults of gearbox effectively.

References

1. Antoni Jérôme, Randall R B. The spectral kurtosis: application to the vibratory surveillance and diagnostics of rotating machines, *Mechanical Systems and Signal Processing* 2006; 20(2): 308-331, <https://doi.org/10.1016/j.ymssp.2004.09.002>.
2. Bechhoefer E, Kingsley M. A Review of time synchronous average algorithms, *Annual Conference of the Prognostics and Health Management Society* 2009; 1-10.
3. Bobin Jérôme, Starck Jean-Luc, Fadili Jalal M, Moudden Yassir and Donoho David L. Morphological Component Analysis: An Adaptive Thresholding Strategy, *IEEE Transactions on Image Processing* 2007; 16(11): 2675-2681, <https://doi.org/10.1109/TIP.2007.907073>.
4. Garcia R A G, Osornio R R A and Granados L D. Smart sensor for online detection of multiple-combined faults in VSD-Fed induction motors, *Sensors* 2012; 12: 11989-12005, <https://doi.org/10.3390/s120911989>.
5. Gilles Jérôme. Empirical wavelet transform, *IEEE Transactions on Signal Processing* 2013; 61(16): 3999-4010, <https://doi.org/10.1109/TSP.2013.2265222>.
6. Guo Y C, Parker R G. Purely rotational model and vibration modes of compound planetary gears, *Mechanism & Machine Theory* 2010; 45: 365-377, <https://doi.org/10.1016/j.mechmachtheory.2009.09.001>.
7. Haile Mulugeta A, Dykas Brian. Blind source separation for vibration-based diagnostics of rotorcraft bearings, *Journal of Vibration and Control* 2015; 22(18): 3807-3820, <https://doi.org/10.1177/1077546314566041>.
8. He S, Chen J, Zhou Z et. al. Multifractal entropy based adaptive multiwavelet construction and its application for mechanical compound-fault diagnosis, *Mechanical Systems and Signal Processing* 2016; 76-77: 742-758, <https://doi.org/10.1016/j.ymssp.2016.02.061>.
9. Henriquez Patricia, Alonso Jesus B, Ferrer Miguel A, Travieso Carlos M. Review of Automatic Fault Diagnosis Systems Using Audio and Vibration Signals, *IEEE Transactions on Systems, Man, and Cybernetics: Systems* 2013; 44(5): 642-652, <https://doi.org/10.1109/TSMCC.2013.2257752>.
10. Huang N E, Shen Z, Long S R et al. The empirical mode decomposition and the Hilbert spectrum for nonlinear and non-stationary time series analysis, *Proceedings Mathematical Physical & Engineering Sciences* 1998; 454: 903-995, <https://doi.org/10.1098/rspa.1998.0193>.
11. Jiang H, Li C and Li H. An improved EEMD with multiwavelet packet for rotating machinery multi-fault diagnosis, *Mechanical Systems and Signal Processing* 2013; 36(2): 225-239, <https://doi.org/10.1016/j.ymssp.2012.12.010>.
12. Jiang Y, Zhu H, Li Z. A new compound faults detection method for rolling bearings based on empirical wavelet transform and chaotic oscillator, *Chaos, Solitons & Fractals* 2016; 89: 8-19, <https://doi.org/10.1016/j.chaos.2015.09.007>.
13. Khadem S E, Rezaee M. Development of vibration signature analysis using multiwavelet systems, *Journal of Sound and Vibration* 2003; 261(4): 613-633, [https://doi.org/10.1016/S0022-460X\(02\)00992-6](https://doi.org/10.1016/S0022-460X(02)00992-6).
14. Li X, Li J, He D, Qu Y. Gear pitting fault diagnosis using raw acoustic emission signal based on deep learning, *Eksploatacja i Niezawodnosc-Maintenance and Reliability* 2019; 21(3): 403-410, <https://doi.org/10.17531/ein.2019.3.6>.
15. Li Z, Yan X, and Tian Z et al. Blind vibration component separation and nonlinear feature extraction applied to nonstationary vibration signals for the gearbox multi-fault diagnosis, *Measurement* 2013; 46: 259-271, <https://doi.org/10.1016/j.measurement.2012.06.013>.
16. McFadden P D. Interpolation techniques for time domain averaging of gear vibration, *Mechanical Systems and Signal Processing* 1989; 3: 87-97, [https://doi.org/10.1016/0888-3270\(89\)90024-1](https://doi.org/10.1016/0888-3270(89)90024-1).
17. Mirjalili S, Lewis A. The whale optimization algorithm, *Advances in Engineering Software* 2016; 95: 51-67, <https://doi.org/10.1016/j.advengsoft.2016.01.008>.
18. Pan H Y, Yang Y, Li X et al. Symplectic geometry mode decomposition and its application to rotating machinery compound fault diagnosis. *Mechanical Systems and Signal Processing* 2019; 114: 189-211, <https://doi.org/10.1016/j.ymssp.2018.05.019>.
19. Purushotham V, Narayanan S, Prasad Suryanarayana A N. Multi-fault diagnosis of rolling bearing elements using wavelet analysis and hidden Markov model based fault recognition, *NDT & E International* 2005; 38 (8): 654-664, <https://doi.org/10.1016/j.ndteint.2005.04.003>.
20. Rashid H S J, Place C S, Mba D, Keong R L C, Healey A, Kleine-Beek W, Romano M. Reliability model for helicopter main gearbox lubrication system using influence diagrams, *Reliability Engineering & System Safety* 2015; 159: 50-57, <https://doi.org/10.1016/j.res.2015.01.021>.
21. Seshadrinath Jeevanand, Singh Bhim, Panigrahi Bijaya Ketan. Investigation of Vibration Signatures for Multiple Fault Diagnosis in Variable Frequency Drives Using Complex Wavelets, *IEEE Transactions on Power Electronics* 2014; 29(2): 936-945, <https://doi.org/10.1109/TPEL.2013.2257869>.
22. Singh Amandeep, Parey Anand. Gearbox fault diagnosis under non-stationary conditions with independent angular re-sampling technique applied to vibration and sound emission signals, *Applied Acoustics* 2019; 144(15): 11-22, <https://doi.org/10.1016/j.apacoust.2017.04.015>.
23. Singh Sandip Kumar, Kumar Sandeep, Dwivedi J P. Compound fault prediction of rolling bearing using multimedia data, *Multimedia Tools and Applications* 2017; 76(18): 18771-18788, <https://doi.org/10.1007/s11042-017-4419-1>.
24. Smith Jonathan S. The local mean decomposition and its application to EEG perception data, *Journal of the Royal Society Interface* 2005; 2: 443-454, <https://doi.org/10.1098/rsif.2005.0058>.
25. Tabrizi A, Garibaldi L, Fasana A, Marchesiello S. Early damage detection of roller bearings using wavelet packet decomposition, ensemble empirical mode decomposition and support vector machine, *Meccanica* 2015; 50(3): 865-874, <https://doi.org/10.1007/s11012-014-9968-z>.
26. Teng W, Ding X and Zhang X et al. Multi-fault detection and failure analysis of wind turbine gearbox using complex wavelet transform, *Renewable Energy* 2016; 93: 591-598, <https://doi.org/10.1016/j.renene.2016.03.025>.

27. Wang Q, Chen H, Chen X, Yang H, Wang G. Early fault detection of gearbox using weak vibration signals, *Eksploatacja i Niezawodnosc-Maintenance and Reliability* 2011; 1(49): 11-15.
28. Wang Y, He Z, Zi Y. Enhancement of signal denoising and multiple fault signatures detecting in rotating machinery using dual-tree complex wavelet transform, *Mechanical Systems and Signal Processing* 2010; 24 (1): 119-137, <https://doi.org/10.1016/j.ymssp.2009.06.015>.
29. Wu Z, Huang N E. Ensemble empirical mode decomposition: a noise-assisted data analysis method, *Advances in Adaptive Data Analysis* 2011; 1(01): 1-41, <https://doi.org/10.1142/S1793536909000047>.
30. Yu D, Wang M, Cheng X. A method for the compound fault diagnosis of gearboxes based on morphological component analysis, *Measurement* 2016; 91: 519-531, <https://doi.org/10.1016/j.measurement.2016.05.087>.
31. Zibulevsky Michael, Zeevi Yehoshua Y. Extraction of a source from multichannel data using sparse decomposition, *Neurocomputing* 2002; 49(1-4): 163-173, [https://doi.org/10.1016/S0925-2312\(02\)00515-5](https://doi.org/10.1016/S0925-2312(02)00515-5).
32. Zosso D, Dragomiretskiy K. Variational Mode Decomposition. *IEEE Transactions on Signal Processing* 2014; 62(3): 531-544, <https://doi.org/10.1109/TSP.2013.2288675>.
33. Zuber N, Bajric R, Sostakov R. Gearbox faults identification using vibration signal analysis and artificial intelligence methods. *Eksploatacja i Niezawodnosc-Maintenance and Reliability* 2014; 16: 61-65.

Xin ZHANG

Jianmin ZHAO

Army Engineering University, Shijiazhuang, China

E-mail: Xinzhang91@hotmail.com, jm_zhao@hotmail.com
